Organic & Biomolecular Chemistry

Accepted Manuscript

This article can be cited before page numbers have been issued, to do this please use: F. M. Cabrerizo, J. G. Yañuk, M. P. Denofrio, F. A. O. Rasse-Suriani, F. D. Villarruel, F. Fassetta, F. S. García Einschlag, R. Erra-Balsells and B. Epe, *Org. Biomol. Chem.*, 2018, DOI: 10.1039/C8OB00162F.

This is an Accepted Manuscript, which has been through the Royal Society of Chemistry peer review process and has been accepted for publication.

Accepted Manuscripts are published online shortly after acceptance, before technical editing, formatting and proof reading. Using this free service, authors can make their results available to the community, in citable form, before we publish the edited article. We will replace this Accepted Manuscript with the edited and formatted Advance Article as soon as it is available.

You can find more information about Accepted Manuscripts in the author guidelines.

Please note that technical editing may introduce minor changes to the text and/or graphics, which may alter content. The journal's standard Terms & Conditions and the ethical guidelines, outlined in our author and reviewer resource centre, still apply. In no event shall the Royal Society of Chemistry be held responsible for any errors or omissions in this Accepted Manuscript or any consequences arising from the use of any information it contains.

ROYAL SOCIETY OF CHEMISTRY

rsc.li/obc

View Article Online
DOI: 10.1039/C8OB00162F

DNA DAMAGE PHOTO-INDUCED BY CHLOROHARMINE ISOMERS: HYDROLYSIS VERSUS OXIDATION OF NUCLEOBASES

Juan G. Yañuk [a], *M. Paula Denofrio* [a], *Federico A. O. Rasse-Suriani* [a, b], *Fernando D. Villarruel* [a, b], *Federico Fassetta* [a], *Fernando S. García Einschlag* [b], *Rosa Erra-Balsells* [c], *Bernd Epe* [d] *and Franco M. Cabrerizo* [a,]*

[a] Instituto Tecnológico de Chascomús (INTECH), Universidad Nacional de San Martín (UNSAM) - Consejo Nacional de Investigaciones Científicas y Técnicas (CONICET), Intendente Marino Km 8.2, CC 164 (B7130IWA), Chascomús, Argentina. E-mail: fcabrerizo@intech.gov.ar

[b] INIFTA - CONICET, Universidad Nacional de La Plata, Diag. 113 y 64, (1900) La Plata, Argentina.

[c] CIHIDECAR - CONICET, Departamento de Química Orgánica, Facultad de Ciencias Exactas y Naturales, Universidad de Buenos Aires, Pabellón 2, 3p, Ciudad Universitaria, (1428) Buenos Aires, Argentina.

[d] Institute of Pharmacy and Biochemistry, University of Mainz, Staudingerweg 5, Mainz, Germany.

* To whom correspondence should be addressed (fcabrerizo@intech.gov.ar)

View Article Online
DOI: 10.1039/C8OB00162F

ABSTRACT

Photodynamic therapy (PDT) is an emerging clinical treatment currently used against a wide range of both cancerous and noncancerous diseases. The search of new active photosensitizers as well as the development of novel selective delivery systems are the major challenges faced by PDT. We investigated herein three chloroharmine derivatives (6-, 8- and 6,8-dichloroharmine) with quite promising intrinsic photochemical tuneable properties and their capability to photoinduce DNA damage in order to elucidate the underlying photochemical mechanisms. Data revealed that the three compounds are quite efficient photosensitizers. The overall extent of photo-oxidative DNA damage induced by both 8-chloro-substituted β-carbolines is higher than that induced by 6-chloro-harmine. The predominant type of lesions generated also depends on the position of the chlorine atom in the β-carboline ring. Both 8-chloro-substituted β-carbolines mostly oxidize purines via type I mechanism, whereas 6-chloro-harmine mainly behaves as a "clean" artificial photonuclease inducing single-strand breaks and site of base loss via proton transfer and concerted (HO^- -mediated) hydrolytic attack. The latter finding represents an exception to the general photosensitizing reactions and, to the best of our knowledge, this is the first time that this process is well documented. The controlled and selective production of different oxygen-independent lesions could be fine-tuned by simply changing the substituent groups in the β-carboline ring. This could be a promising tool for the design and development of novel photo-therapeutic agents aimed to tackle hypoxic conditions shown in certain types of tumours.

Keywords: DNA hydrolysis, DNA photosensitization, β-carbolines, photonuclease, MCR-ALS algorithm

View Article Online
DOI: 10.1039/C8OB00162F

INTRODUCTION

Photodynamic therapy (PDT) is a widely used treatment against both cancerous and noncancerous diseases, based on the cytotoxicity of photosensitizers in the presence of light [1, 2]. Two-photon photodynamic therapy (TPA-PDT) represents a novel variation of PDT currently under pre-clinical investigation [3, 4]. These facts have led, not only to an actively seeking of new active photosensitizers, but also of novel selective delivery systems. Increased selectivity and effectiveness of the treatment is expected if a specific uptake of the photosensitizers into the target cells, often tumor cells, can be achieved.

For a successful clinical trial, PDT agents should be provided with a set of intrinsic and unique photophysical characteristics. In this context, β-carboline alkaloids (βCs) could represent an alternative to be explored. βCs are a group of highly biocompatible photoactive compounds, derived from the structural unit 9H-pyrido[3,4-b]indole or *nor*harmane. βCs show several unique properties such as high chemical and photochemical stability [5-8]. Upon one- (OPA) and two-photon (TPA) excitation, βCs can produce non-negligible quantities of singlet molecular oxygen ($^1O_2$), as well as other reactive oxygen species ($O_2^{\bullet-}$ and H_2O_2) [5-10]. Most of them also show high fluorescence quantum yields [5-8]. Moreover, these alkaloids have been shown to be efficient photosensitizers [10-18], even under intracellular conditions [16, 17] and/or when loaded in microporous coordination polymers [18]. All these intrinsic chemical properties make them suitable for PDT and TPA-PDT.

From the chemical point of view, βCs are quite versatile molecules. These alkaloids can be subjected to multiple chemical transformations to fine tune their physicochemical properties and/or to further coordinate (or conjugate) them with transition metals [19, 20] or macromolecular carriers (such as proteins) [17] that can provide selective drug-uptake into the target cells. Furthermore, due to their relative low molecular weight, several βC-molecules can be loaded and/or conjugated per carrier structure. In a very recent study we have demonstrated that albumin–folate conjugates appear to be promising selective vehicles for a tumor cell targeted PDT, making use of the folic acid receptor α (FRα), which is overexpressed on the surface of many tumor cells and mediates an endocytotic uptake [17]. In this case, two particular βCs were used as photoactive (*i.e.*, photosensitizers and/or fluorescence markers) drugs covalently linked to folate-tagged albumin as a selective carrier system. Although encouraging results were obtained, the overall photodynamic efficiency was relatively low. This fact could be a consequence of an overload of the overall uptake process (*i.e.*, FRα expression, binding, endocytosis and FRα recycling) and/or due to a poor efficiency of the photosensitizer used.

View Article Online
DOI: 10.1039/C8OB00162F

In the search of novel photosensitizers based on small molecules that can be more effective at low doses, absorbing in the far UVA and/or visible region, we investigated herein the capability of three chloroharmine derivatives (Scheme 1) to photoinduce DNA damage. The target model was chosen due to its high reactivity and multiple attack sites (Scheme 2a), via different chemical and photochemical pathways, giving rise to the formation of a very broad spectrum of photoproducts (Scheme 2b) [21]. Thus, in a single model, different photosensitizers that may have different mechanisms of action can be evaluated. *I.e.*, type I (hydrogen abstraction and electron transfer reactions) and type II (via singlet oxygen) photooxidation, triplet-triplet energy transfer, catalyzed-hydrolytic attack, alkylation and/or reactivity of π-bonds or C-H bonds of DNA bases with radical intermediates ($HO^{\bullet}$, $Cl^{\bullet}$, among others) [21-26]. The advantage of this model is that it is simple and provides valuable information regarding the extent and the molecular bases of the photosensitized processes involved. On the other hand, chloroharmines were selected because of the relatively high intrinsic photosensitizing efficiency of harmine rings system and the bathochromic shift induced by chloro-substituents, giving rise to absorption in the UVA and visible range of the spectrum [7]. Moreover, chloro-harmines were shown to be involved in two-photon excitation processes yielding, in consequence, the population of their respective photoexcited states [6, 27], with the concomitant TPA-photosensitized singlet oxygen ($^1O_2$) formation [5]. These facts make chloro-substituted βCs excellent candidates that deserve to be investigated.

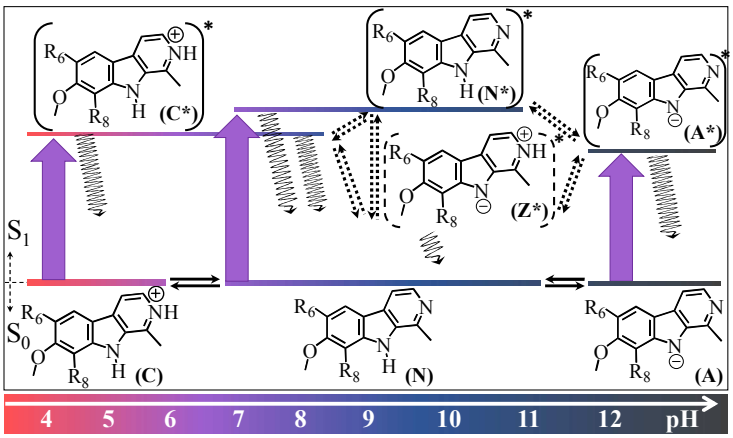

Scheme 1. Structures of the investigated compounds Ha (R_6 = R_8 = H), 6-Cl-Ha (R_6 = Cl and R_8 = H), 8-Cl-Ha (R_6 = H and R_8 = Cl) and 6,8-diCl-Ha (R_6 = R_8 = Cl), and dominant acid-base equilibria present in aqueous media, in the whole pH range investigated. Drawings represent the dominant acid-base species present as a function of the pH according to the scale at the bottom (C = Cation, N = Neutral, Z = zwitterion, and A = Anion). Black solid and dashed arrows indicate processes or equilibria taking place in the ground (S_0) (C, N and A) and first (S_1) (C*, N*, Z* and A*) electronic excited states, respectively.

View Article Online
DOI: 10.1039/C8OB00162F

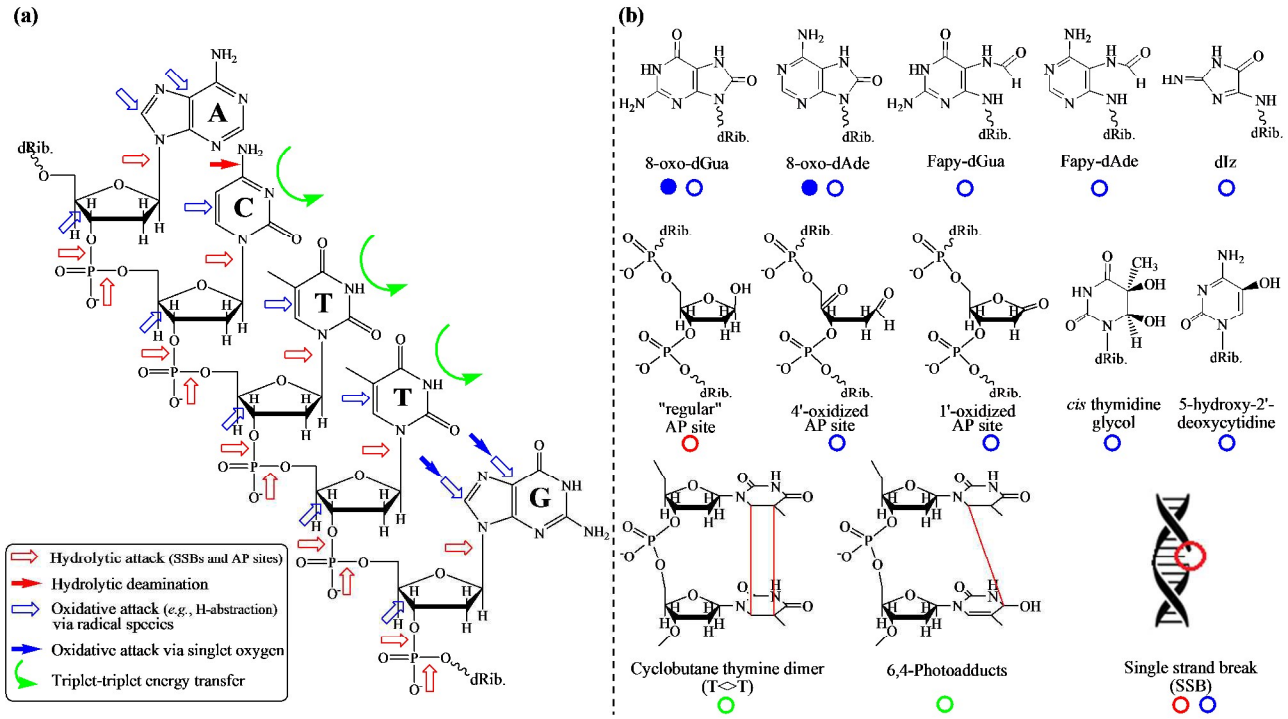

Scheme 2. (a) DNA's most probable attack sites. **(b)** Chemical structures of the most representative DNA modifications induced by photosensitization. Inset shows the color convention used to indicate different reactions' types. Reactivity sites and the types of products formed are pointed by arrows and circles, respectively.

EXPERIMENTAL

General

Reactants: harmine (Ha, Sigma-Aldrich, > 98%) was used without further purification. The method used to synthesize and purify the three chloroharmine derivatives (6-Cl-Ha, 8-Cl-Ha and 6,8-diCl-Ha) has been published elsewhere [28]. DNA from bacteriophage PM2 (PM2 DNA, 10^4 bp) was prepared according to the method of Salditt *et. al.*[29] Calf thymus DNA (ctDNA), provided by Sigma-Aldrich, was dissolved in Tris (10 mM) with EDTA (1 mM) at pH 7.5 – 8.0.

Enzymes: Formamidopyrimidine-DNA glycosylase (Fpg protein) was obtained from *E. coli* strain JM105 harboring plasmid pFPG230 [30]. Endonuclease IV and T4 endonuclease V were partially purified from an inducible overproducer (*E. coli* strain A 32480 carrying the plasmid ptac-denV) provided by L. Mullenders, Leiden. Endonuclease III from E. coli was kindly provided by S. Boiteux, Fontenay aux Roses, France. All repair endonucleases were tested for their incision at reference modifications (*i.e.*, thymine glycols induced by OsO_4, AP sites by low pH and cyclobutane pyrimidine dimers, CPDs, by UV254) under the applied assay conditions (*vide infra*) to ensure that the correct substrate modifications are fully recognized and no incision at non-substrate

View Article Online
DOI: 10.1039/C8OB00162F

modifications takes place [31]. Superoxide dismutase (SOD) and catalase were from Sigma-Aldrich.

pH adjustment: The pH of βC derivatives aqueous solutions was adjusted by adding drops of aqueous NaOH or HCl solutions (concentration ranged from 0.1 to 2.0 M) with a micropipette. The ionic strength was approximately 10^{-3} M in all the experiments. In experiments using deuterated material, D_2O (> 99.9%; Sigma), DCl (99.5%; Aldrich) and NaOD (Aldrich) were used. The pD of the solution was adjusted as it was described elsewhere [33], the final isotope purity was greater than 96%. Buffered βC acidic, neutral and alkaline solutions were prepared in acetic acid–sodium acetate (pH 4.8, 100 mM), KH_2PO_4–NaOH (pH 7.4, 50 mM) and $Na_2B_4O_7$–NaOH (pH 10.0, 12.5 mM) buffers, respectively.

Binding studies

The interaction of βC derivatives with ctDNA was studied by both UV-visible absorption and fluorescence spectroscopy. Equipment and data analysis used were described elsewhere [10]. For the analysis of the recorded absorption, emission or excitation spectra, we applied bilinear resolution techniques as recently described [8]. Briefly, estimates of the contributing spectral profiles were retrieved from each data matrix $D_X(i \times j)$ by applying the popular alternating least-squares (ALS) algorithm [32]. The latter deconvolution is based on the iterative application of the following matrix product: $D_X = CS_X^T + E$, where $C(i \times n)$ are the matrices of contribution profiles; $S_X^T(n \times j)$ are those containing the desired spectral profiles and $E(i \times j)$ represent the unexplained variances. The indexes n and j denote the number of independent contributions and the spectral wavelengths, respectively, whereas the i indexes define the experimental conditions associated to each recorded spectrum. During the deconvolution processes, rotational and scale ambiguities [33] were reduced by imposing non-negativity and unimodality constraints [34]. An averaged molar absorption coefficient at 260 nm ($\varepsilon^{260\ nm}$) of 18500 (M, in bp)$^{-1}$ cm^{-1} was used to calculate the [DNA] of the stock solutions.

DNA photoproducts characterization

Irradiation set-up. A mixture of βC buffered aqueous solutions (10 mM KH_2PO_4, 50 mM NaCl, pHs 5.5, 7.2, 7.4, 8.1 and 8.7, as appropriate) and PM2 DNA (at 10 μg/ml) were irradiated for 20 min on ice in a 96 well-plate with a UVA Philips HPW 125W lamp emitting at 365 (± 20) nm, placed at a distance of 10 cm. Treated DNA was precipitated by ethanol/sodium acetate and, then, dissolved in BE1 buffer (20 mM Tris–HCl, pH 7.5; 100 mM NaCl and 1 mM EDTA) for damage analysis.

View Article Online
DOI: 10.1039/C8OB00162F

Quantitative analysis of endonuclease-sensitive modifications. The DNA relaxation assay used to quantify the number of photoinduced endonuclease-sensitive sites (ESS) and single-strand breaks (SSB) in PM2 DNA has been described earlier [21, 35]. It makes use of the fact that supercoiled PM2 DNA is converted by either a SSB or the incision of a repair endonuclease into a relaxed (nicked) form, which migrates separately from the supercoiled form in agarose gel electrophoresis. Its application to characterize the DNA damage induced by photosensitization as well as the type of repair enzymes and experimental conditions have been previously described in detail [10].

RESULTS

Photosensitization of cell-free DNA by chloroharmines

Dose-dependence of the DNA damage induced by photoexcited chloroharmines

Supercoiled DNA of bacteriophage PM2 was exposed to UVA (365 nm) irradiation in the presence of different concentrations of chloroharmines in phosphate buffered (pH 7.4) solutions. The number of single-strand breaks (SSBs), as well as DNA modifications recognized by the DNA repair glycosylase Fpg [*i.e.*, oxidized purines and sites of base loss (AP sites)] were subsequently quantified. As observed in previous studies for other related βCs [10, 14, 16], the number of DNA modifications increases with the compounds' concentration (Figure 1a). All the damage is mediated by the photoexcited βC derivatives, since no damage was observed in both *light-controls* (PM2 DNA irradiated in the absence of chloroharmines, see data points at the y-intercept in Figure 1a) and *dark-controls* (mixtures of PM2 and chloroharmines, at the highest concentrations, kept in the dark) (Figure SI.1a).

The type and extent of DNA-damage depend upon the position of the chlorine atom in the βC's ring. In the case of Ha, 8-Cl-Ha and 6,8-diCl-Ha, Fpg-sensitive sites prevail over SSBs by a factor of 3, 4 and 10, respectively. Surprisingly, the number of SSBs induced by 6-Cl-Ha is clearly higher than Fpg-sensitive base modifications (factor of SSBs over Fpg-sensitive sites of ~ 3). This is a quite unique behaviour among all the βCs investigated [10, 14, 16]. Both 8-chloro-substituted βCs were shown to be more efficient photosensitizers than 6-Cl-Ha and Ha. In particular, 6,8-diCl-Ha was 20-, 170- and 290-fold more potent as damaging agent than 8-Cl-Ha, 6-Cl-Ha and Ha, respectively, in the case of the Fpg-sensitive sites, and 10-, 5- and 80-fold, respectively, in the case of the SSBs (ratios calculated from the linear slopes of the concentration-dependent data depicted in Figure 1).

SSBs can be produced not only by a direct catalytic hydrolysis on the phosphodiester bond

View Article Online
DOI: 10.1039/C8OB00162F

(Scheme 2), but also as a consequence of secondary reactions from Fpg-sensitive sites. Although under physiological conditions these reactions are extremely slow, thermal workup, sodium hydroxide, or treatment with various amines facilitate strand cleavage at AP sites [22]. Linearity on both SSBs and Fpg-sensitive sites shown in Figure 1a allow us to dismiss secondary reactions. This is further supported by the time-dependence study shown in Figure 1b and in Supporting Information Figure SI.1b and c. For comparison, the time-dependence for 6,8-diCl-Ha was also determined. In the case of 6-Cl-Ha, the prevalence of SSBs was observed for all the irradiation times tested. Thus, DNA damage induced by photoexcited chloroharmines occurs through, at least, two independent photosensitizing pathways (*vide infra*).

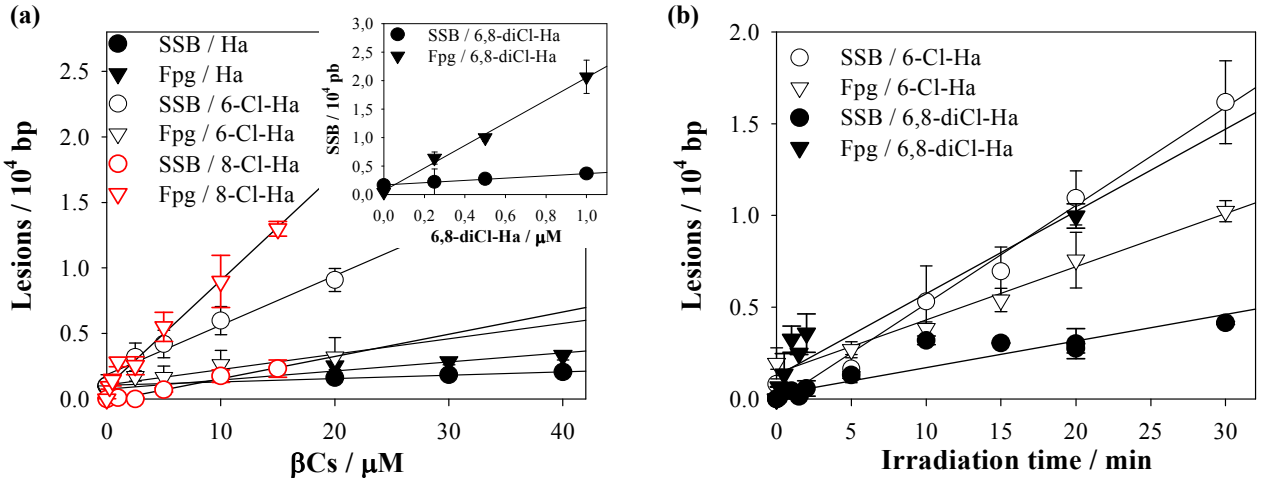

Figure 1. (a) SSBs and modifications sensitive to Fpg protein induced in PM2 DNA by exposure to UVA (365 (± 20) nm, 20 min) in the presence of different concentrations of chloroharmine phosphate buffer solutions (pH 7.4). **(b)** Time-dependence of the damage induced by 6-Cl-Ha (20 μM) and 6,8-diCl-Ha (0.5 μM). Data are the mean of 4 independent experiments (± S.D).

Quantification of endonuclease-sensitive modifications in PM2 plasmid: DNA damage profiles

Photosensitization can lead to the formation of a wide range of DNA photoproducts. Thus, the number of various other types of repair enzyme-sensitive modifications induced by the photoexcited chloroharmines in phosphate pH 7.4 buffer, were also determined (Figure 2). Each repair endonuclease used recognizes different DNA modifications: *Fpg-protein (Fpg)* recognizes both oxidized purines such as 8-oxoG and AP sites [36], *endonuclease III (Endo III)* detects various oxidized pyrimidines as well as AP sites, *T4 endonuclease V (T4 endo V)* recognizes cyclobutane pyrimidine dimers (CPDs) together with some types of AP sites, and *endonuclease IV (Endo IV)* recognizes all types of sites of base loss, including all types of oxidized AP sites. Therefore, the amount of CPDs (named $CPDs^{calc}$) produced upon photoexcitation is calculated as the difference

View Article Online
DOI: 10.1039/C8OB00162F

between number of sites recognized in the incubation with both *Endo IV* and *T4 endo V* and the number of AP sites recognized by *Endo IV* alone. In addition, a similar analysis based on data obtained from the combination of both *Endo III* and *Endo IV* enzymes is performed to estimate the number of oxidative damage induced on pyrimidinic nucleobases (named Ox-Py^{calc}).

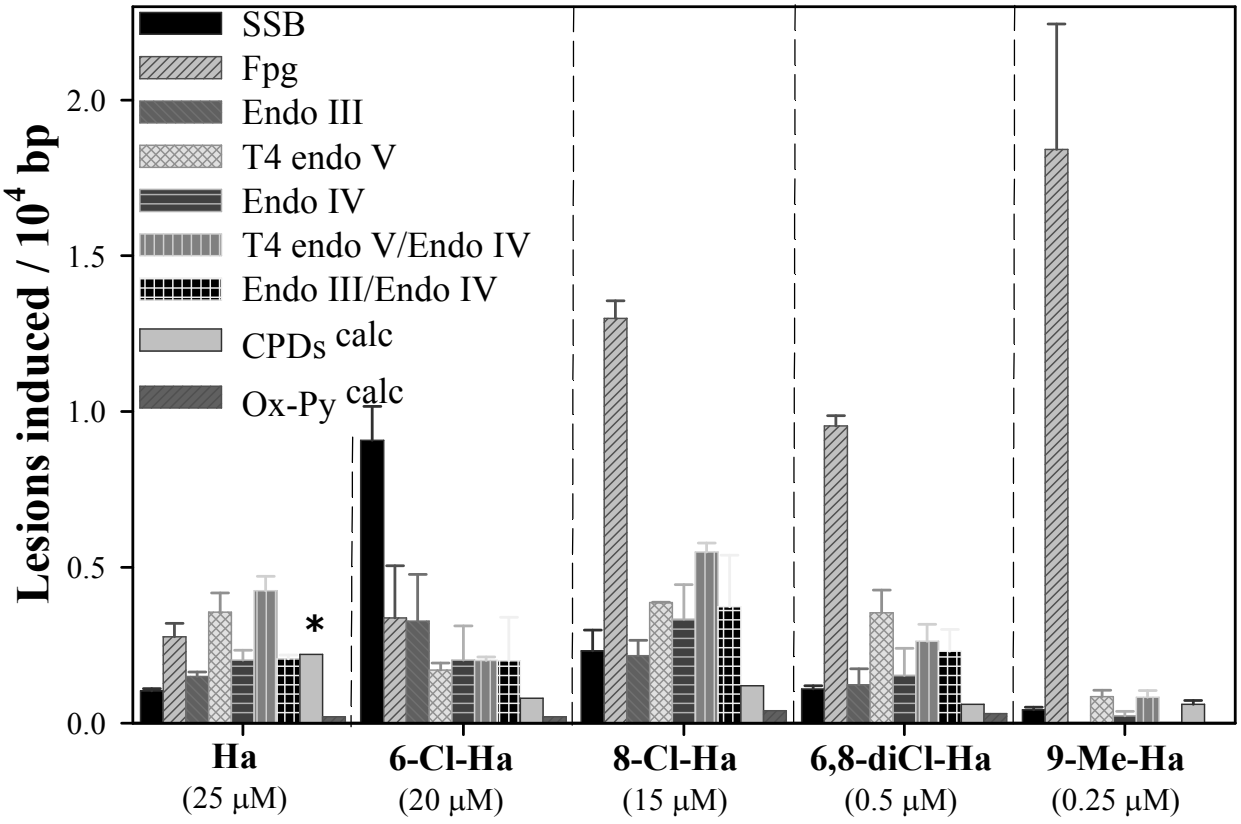

Figure 2. DNA damage profiles showing SSB and several endonuclease sensitive modifications induced in PM2 DNA by photo-excited (UVA 365 (± 20) nm) chloroharmines. Data shown for Ha and 9-methyl-harmine (9-Me-Ha) were taken from references [16] and [10], respectively. Data are the mean of 3 independent experiments (± S.D).

From the data shown in Figure 2, four major points deserve to be highlighted:

(i) Contrary to the results previously obtained with Ha [14], no CPDs^{calc} were detected when chloroharmines were used as photosensitizers. Note that DNA photosensitization can lead to the formation of different types of CPDs such as thymine-thymine (TT), thymine-cytosine (TC), cytosine-thymine (CT) and cytosine-cytosine (CC) dimers [37] . Nevertheless, TT clearly contributes the most to the total CPDs number (~70% – 90%). With the exception of CC [38], CPDs are formed through triplet-triplet energy transfer (TTET) from the triplet electronic excited state of the photosensitizer to the triplet electronic state of thymine base (giving rise to the formation of locally excited pyrimidine triplet states) and/or to thymine base in, at least, a dinucleotide arrangement (resulting in the formation of delocalized triplet excited states) [37, 39]. In DNA, the latter process is

View Article Online
DOI: 10.1039/C8OB00162F

thermodynamically favoured when absorbing chromophores having energy triplet values (E_T) larger than 267 kJ/mol are used as photosensitizers [40]. Thus, with the exception of neutral 6,8-diCl-Ha, with E_T = 275.6 kJ/mol [7], neither the triplet state of protonated 6,8-diCl-Ha nor both acid-base species of 6-Cl-Ha and 8-Cl-Ha have the required energy to generate cyclobutane thymidine dimers (*i.e.*, 248.7 kJ/mol < $E_T^{chloroharmines}$ < 253.5 kJ/mol) [7]. In the particular case of neutral 6,8-diCl-Ha, although triplet-triplet energy transfer processes would be favourable from the thermodynamic point of view, the absence of $CPDs^{calc}$ might be explained either by its rather low absorption coefficient (*vide infra*) and/or by the quite efficient quenching of βCs' triplet states by molecular oxygen (k_q = 2.41 x 10^9 M^{-1} s^{-1}) [7], which leads to a decrease on the stationary triplet-state concentration. Moreover, a weak non-covalent interaction of the neutral species with DNA[13, 14] might also contribute to a lower efficiency of CPDs formation (*vide infra*).

(ii) No measurable oxidatively generated damage on pyrimidine bases ($Ox\text{-}Py^{calc}$) was induced by the four photosensitizers investigated. It is well-known that the reactivity of pyrimidine bases with most ROS including singlet oxygen, superoxide anion radical and hydrogen peroxide, at the exception however of hydroxyl radical ($HO^{\bullet}$) is quite inefficient [41]. In addition to $HO^{\bullet}$-mediated reactions, pyrimidine bases can be part of one-electron photosensitized oxidative reactions, as it was demonstrated for the epigenetic modification 5-methyl-2'-deoxycytidine [42, 43]. Therefore, results shown in Figure 2 indirectly suggest that highly reactive radical species, that might be formed by photodegradation of chloroharmines [7], do not play a key role in the overall DNA oxidative damage (*vide infra*). Moreover, data also suggest that, under our experimental conditions, chloroharmines would not have the required redox potential to photo-induce pyrimidine oxidations.

(iii) The damage profiles of all three chloroharmines differ considerably from that of unsubstituted Ha. Briefly, while Ha induces a broad-spectrum profile with the presence of several types of photoproducts (oxidized purines, AP sites and CPDs), chloroharmines appear more selective. Interestingly, the predominant type of lesion generated depends on the position of the chlorine atom in the βC's ring: *i.e.*, both 8-Cl-Ha and 6,8-diCl-Ha induce mostly Fpg-sensitive purine modifications, whereas 6-Cl-Ha predominantly induces SSBs. As mentioned above, the latter finding is quite unique in comparison not only to the compounds investigated herein, but also to all the βCs previously studied (Figure 2) [10, 14, 16].

(iv) The overall extent of photo-oxidative DNA damage induced by 8-chloro-substituted βCs is the highest (*i.e.*, lower doses of 8-Cl-Ha and 6,8-Cl-Ha had to be applied to induce a similar extent of oxidative damage as induced by Ha or 6-Cl-Ha).

View Article Online
DOI: 10.1039/C8OB00162F

The differences described above could result from differences in the chemical, photochemical and/or photophysical reactivity of the chloroharmines (*i.e.*, distinctive efficiency of ROS production, etc.). The presence of a chlorine atom as substituent at C-8 in 8-Cl-Ha and 6,8-diCl-Ha could also have an important stereo-electronic effect on the NH indolic moiety (Scheme SI.1 in Supplementary Information). In consequence, the lack of this effect in 6-Cl-Ha might induce a distinctive photosensitizing behavior. Also, a difference on the mode and strength of their non-covalent interaction with DNA could account for the above mentioned observations, as it was suggested for other related heterocyclic compounds [44]. All these aspects are further explored and discussed in the following sections.

Thermal stability of chloroharmines in phosphate (pH 7.4) buffer

In aqueous low-alkaline solutions (pH > 7.4) 8-Cl-Ha and 6,8-diCl-Ha are subject to a quite fast and irreversible chemical decomposition [7]. The short distance between the chlorine atom and the indolic-NH group in both 8-chloro-substituted βCs would account for the formation of an intramolecular hydrogen-bridge-like interaction yielding in a higher rate of reaction. Then a putative product might be responsible for the high damaging effect observed for these two particular photosensitizers.

In order to characterize this reaction in more detail, the chemical stability of 8-chloroharmines in phosphate buffer (pH 7.4) was monitored by UV-vis absorption spectroscopy and HPLC (Figure SI.2). Under this condition, both compounds were stable when stored in the dark during the time-window of the experiments. In consequence, thermal decomposition does not account for the high photosensitizing activity of 8-chloroharmines described above. Instead, different binding affinities and/or different capabilities of ROS production might play a key role (*vide infra*).

Role of reactive oxygen species (ROS)

Photo-reactivity of βCs with biomolecules such as DNA and 2'-deoxynuecleotide 5'-monophosphates has been well documented [10-14, 16, 17]. The established mechanisms mostly involve electron transfer reactions between the first electronic excited state of the protonated βC derivatives ($^1[\beta CH^+]^*$) and DNA-nucleobases (*i.e.*, by a direct type I photoreaction). ROS do not play a key role in the overall photooxidative damage. In this context, the expectation that ROS do not have a key role in the generation of DNA damage profile shown in Figure 2 is supported by intrinsic

View Article Online
DOI: 10.1039/C8OB00162F

photophysical data of chloroharmines, in particular ***(i)*** their extremely low efficiency of ROS photosensitized generation (Table 1) and ***(ii)*** the observation that quantum yields of ROS produced by chloroharmines do not correlate with the extent of DNA photooxidation depicted in Figures 1 and 2: 6,8-diCl-Ha, which has the lowest ROS production efficiency (in terms of singlet oxygen, $^1O_2$), induces the highest yields of DNA photooxidation.

6-Cl-Ha was further analysed because of the specific damage profile induced by this compound after photoexcitation. It is very unlikely that $^1O_2$ contributes to the observed high yield of SSBs formation. It is commonly accepted that phosphodiester bonds are not the primary target of $^1O_2$. This is supported herein by the lower rate of SSBs generated by two quite efficient $^1O_2$ photosensitizers (*i.e.*, perinaphthenone-2-sulfonic acid in D_2O with $\Phi_\Delta = 0.97 \pm 0.06$ [45] and Rose Bengal in D_2O with $\Phi_\Delta = 0.75$ [46]) compared to that photoinduced by Ha in acidic (pH 4 - 5) D_2O with $\Phi_\Delta = 0.22 \pm 0.02$ [6-8] (Figure SI.3).

In addition to $^1O_2$ ($\Phi_\Delta = 0.19$), UVA excitation of 6-Cl-Ha has been described to generate other ROS such as H_2O_2, $O_2^{\bullet-}$, $HO^\bullet$ as well as other radicals including $\beta C^\bullet$ and $Cl^\bullet$, although with very low efficiency. These species may certainly induce both nucleobase oxidation and/or SSB formation, upon nucleobases hydroxylation or hydrogen abstraction from the deoxyribose ring (Scheme 2, blue-empty arrows). [24]. Therefore, we analysed the contribution of these species in the production of SSBs and Fpg-sensitive sites lesions in two independent types of experiments based on the principle of: *(i) solvent effect*, where the role of $^1O_2$ was investigated by comparing the damage extent and profile observed in H_2O and D_2O buffer solutions as described elsewhere [5], and *(ii) selective ROS scavenging,* by adding SOD, catalase, isopropanol or *tert*-butanol as selective scavengers of $O_2^{\bullet-}$, H_2O_2 and radical species, respectively [5, 14].

Data depicted in Figure 3 clearly show that none of the above-mentioned ROS have a relevant role in the generation of both SSBs and Fpg-sensitive modifications. Only a small increase in the number of Fpg-sensitive sites (*i.e.*, oxidised purine nucleobases, which are known to be the major product from the reaction of DNA with $^1O_2$) was observed in the experiments performed in deuterated water, where $^1O_2$ steady-state concentration is enhanced. On the other hand, having in mind the extremely high and unspecific reactivity of hydroxyl radicals, the lack of oxidative damage on pyrimidine bases (Figure 2) is indicative of the fact that hydroxyl radicals do not play a key role not only in the SSBs formation but also in the overall DNA damage. Therefore, other mechanisms (*e.g.*, concerted hydrolytic attack involving proton (H^+) transfer and OH^- hydrolytic reactions) must be responsible for SSBs formation induced by photoexcited 6-Cl-Ha (*vide infra*). Note that, upon

View Article Online
DOI: 10.1039/C8OB00162F

photoexcitation, βCs induce a drastic change in the local pH.

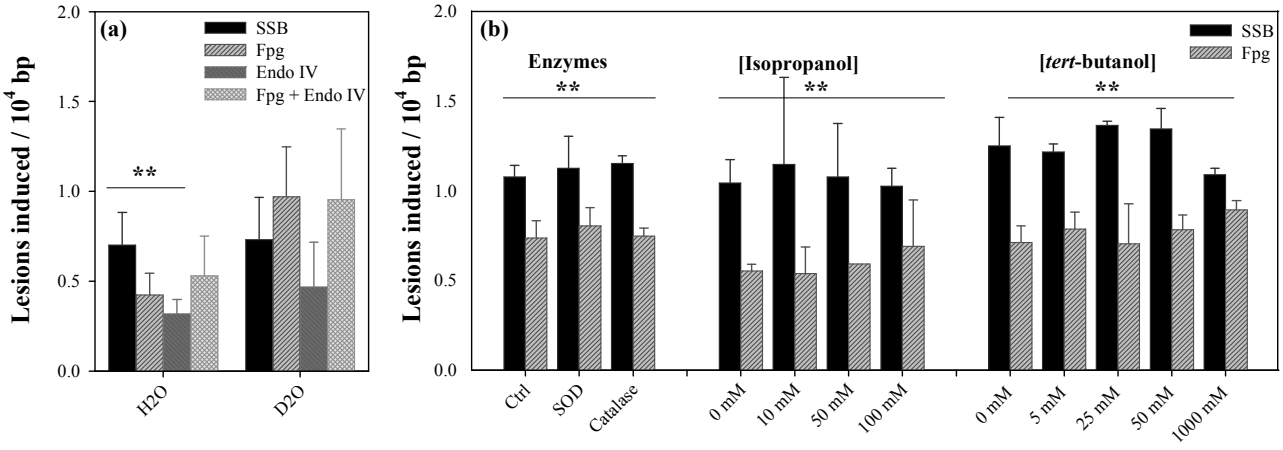

Figure 3. SSB and endonucleases sensitive modifications induced in PM2 DNA by photo-excited 6-Cl-Ha (20 μM) exposure to 20 min of UVA (365 (± 20) nm) light in: **(a)** H_2O and D_2O aqueous media at pH and pD 7.2 and **(b)** H_2O solutions at pH 7.4, in the presence of selective ROS scavengers. All data depicted are the mean of 3 independent experiments (± S.D). * indicates statistically significant differences in each DNA modifications (SSBs or Fpg) between samples irradiated in the presence of scavengers and their corresponding controls ($p < 0.05$, ANOVA / Dunnett´s tests). ** indicates statistically significant differences between SSBs and Fpg-sensitive modifications within each experimental condition ($p < 0.05$, t-tests).

Spectroscopic behaviour of chloroharmines in the absence and in the presence of DNA

In order to elucidate the interaction of chloroharmines with DNA, a series of spectroscopic studies were carried out. In this context, the chemical nature as well as relative distribution of the acid-base species of chloroharmines present in both ground (S_0) and first electronic excited (S_1) states were fully characterized both in the presence and in the absence of DNA

UV-visible absorption and fluorescence emission spectroscopy: effects of solvent and pH.

The influence of the environment (solvents, pH, [O_2], ionic strength, etc.) on the photochemical and photophysical properties of βCs has been well documented [5, 6, 9, 27, 47, 48]. In this context, UV-visible absorption and fluorescence emission spectra of chloroharmines were recorded in buffered air-equilibrated solutions under three different pH conditions: 4.8 (acetate), 7.4 (phosphate) and 8.1 (borax). For comparative reasons, spectra recorded in water were also included.

UV-visible absorption spectra showed the expected qualitative pH-dependence (Figure SI.4). Briefly, **C** is the dominant species (> 99%) when subject to acidic conditions (pH 4.8). The increase of pH yields an increase in the relative concentration of **N**. Thus, under physiological pH conditions (pH 7.4) both **C** and **N** species coexist in the solution (Scheme 1). However, results indicate that a significant amount of **C** is also present under low alkaline conditions (pH 8.1); *i.e.*, ~1.5 pH units

View Article Online
DOI: 10.1039/C8OB00162F

above the pK_a value measured in pure water. The unforeseen presence of **C** may be explained by assuming that the increase in the ionic strength and/or the presence of phosphates and borax salts should stabilize the protonated species of chloroharmines (**C**) resulting in a shift to a higher pH values of the apparent pK_a (pK'_a) value with respect to that observed in pure water [7]. This fact is more evident in the case of 6-Cl-Ha, and the experimental acid-base titration of 6-Cl-Ha in phosphate buffer lead to a pK'_a value of 7.58 ± 0.02 (Figure SI.5). It is worth mentioning that both **N** and **C** have a significant absorption in the region of the excitation source (365 ± 20 nm) used in this work (Figure SI.4). In particular, at pH 7.4, all the investigated compounds have quite similar absorption coefficients at the excitation wavelength (ε^{365nm} ~ 7000 M^{-1} cm^{-1}). In addition, ε^{365nm} decreases with increasing pH. These facts have to be taken into account when comparing the photodynamic effects of chloroharmines (*vide infra*).

Fluorescence emission spectra, recorded in the three buffered solutions, show some qualitative and quantitative differences when comparing with those obtained from pure water (Figure SI.6). Briefly, although the photo-excited cation (**C***) is the main emitting species observed under all three pH conditions (intense broad band centred at 430 nm) [7], the presence of an extra emission band (shoulder centred at ~485 nm) is also evident, even under acidic and low alkaline pH conditions. The latter species, assigned to the electronic excited zwitterion (**Z***) [7], was not observed in acidic pure aqueous solutions [7]. In addition, a less intense pH-dependent emission band, centred at 360 nm, is observed under low alkaline conditions (pH 7.4 and 8.1). Accordingly, this band is assigned to the neutral species from its single excited state (**N***) [7].

These results are consistent with the well-known behaviour of these alkaloids when subject to photo-excitation. Briefly, βCs contain both hydrogen-bonding donor and acceptor groups within their structure (the indolic and pyridinic nitrogen, respectively). Upon excitation, the basicity of the pyridinic- as well as the acidity of the indolic-nitrogen are greatly enhanced. Thus, protonated (**C***) and zwitterionic (**Z***) species might be present due to proton exchange with the solvent [49]. Reyman *et. al.* have recently demonstrated that the rate of protonation (and/or deprotonation) is further enhanced by the presence of proton donor and acceptor groups (*e.g.*, phosphate anions) in the surrounding environment of azaaromatic molecules such as harmane [48]. In this regard, phosphate, acetate and borate anions would have a similar effect on 6-Cl-Ha which might explain the appearance of the emission at ~485 nm.

Results described above also show a distinctive behaviour when comparing with that observed for harmane, another related βC, where **Z*** was not observed in borax buffer solutions [48].

View Article Online
DOI: 10.1039/C8OB00162F

This fact might be a consequence of the change in the electronic distribution of the βC-ring induced by the simultaneous presence of the methoxy and chlorine substituents in chloroharmines and, therefore, in their relative acidity/basicity.

Interactions of chloroharmines with calf thymus DNA (ctDNA)

The interactions between βCs and DNA have long been studied [10-14, 50-52]. Briefly, these alkaloids mainly show a static interaction with DNA leading to the formation of ground-state complexes (^{0}[βC-DNA]). In particular, due to their planar structure, βCs partially intercalate into the DNA double helix with an orientation of the pyridine ring towards the solvent (*i.e.*, towards a protic environment) and/or the negatively charged backbone of DNA [10]. Moreover, βCs are also groove binders and the electrostatic contribution to the overall binding (strength and relative orientation of the interacting molecules) should also be taken into account, when cationic βCs are present in the solutions [10-14]. The presence of two stable interaction modes, minor groove binding and intercalation, was recently confirmed by QM/MM modelling [51, 53, 54]. However, the specific mode and strength of interaction strongly depends on both the chemical structure of the βC and the pH and, as such, has to be investigated separately for every βC derivative.

Titration of chloroharmines with ctDNA was monitored by steady-state fluorescence experiments. In all the cases the increase of ctDNA concentration ([ctDNA]) leads to a significant quenching of chloroharmine's emission (Figure 4, SI.7 and SI.8). With the exception of 6-Cl-Ha at pH 8.2, for all compounds and pH conditions investigated, no change on the corresponding maximum emission wavelength was observed in the entire [ctDNA] range studied. Briefly, a uniform decrease in the spectral region of the three-emitting species is observed as [ctDNA] is increased (see regions I, II and III, for **N***, **C*** and **Z***, respectively). This is better shown in the normalized emission spectra (Figures 4, SI.7 and SI.8). On the contrary, when subject to low-alkaline conditions (pH 8.2), the increase in [ctDNA] induces a clear decrease on the emission of **N*** and **C*** while **Z*** remains constant and/or increases (Figure 4c, insets in *middle column*).

In a qualitative analysis, the above description is in agreement with previous reports regarding the interaction of related βCs with different types of DNA materials [10, 13, 14]. Our findings indicate that neither the protonated nor the neutral species of chloroharmines are fully intercalated into the ctDNA double strand. This is explained by the presence of **C***, even under alkaline conditions, suggesting a polar-protic microenvironment for the βC's pyridine ring [6, 7, 55]. On the other hand, groove binding cannot be ruled out.

View Article Online
DOI: 10.1039/C8OB00162F

In all the cases, the decrease of the fluorescence intensity (I_F, measured as the integral over the entire emission range) as a function of [ctDNA] showed linear Stern–Volmer behaviours (Figures 4, SI.7-SI.9), except for 6-Cl-Ha measured at pH 7.4 and 8.2 showing a negative deviation (downward curvature) to the Stern-Volmer relationship (Figure 4, insets in *right column*, full-black circles). However, Stern-Volmer correlation for I_F^N (*i.e*, fluorescence intensity recorded at the emission maximum of **N***) shows, for both neutral and low-alkaline conditions, a linear behaviour (Figures 4b and 4c, insets in *right column*, full-black squares). The observed deviation is consistent with the fact that the increase of [ctDNA] would result in an increase in the relative concentration of a more efficient emitting species. According to data reported in the previous paragraph, such a species would be **Z*** (or **A***, *vide infra*).

Taking into account the strong static contribution to the ground-state interaction between βCs and DNA described in the literature [10], then, K_{SS} can be considered as an indicative value of the binding constants (K_B) of the ground-state complex formed between the alkaloid and DNA. In this context, when comparing the corresponding Stern-Volmer constants (K_{SS}) listed in Table 1, two clear tendencies were observed: *(i)* the higher the pH, the lower the strength of the interaction observed ($K_{SS}^{(pH\ 4.8)} > K_{SS}^{(pH\ 7.4)} > K_{SS}^{(pH\ 9.5)}$). This is the general behaviour already described for other related compounds [10, 14] and the observed trend can be explained in terms of electrostatic interaction: the lower the pH, the higher the fraction of βC's molecules with positive net charge. This fact leads to a higher interaction with the negatively charged backbone of ctDNA. *(ii)* The presence of chlorine atoms slightly increases the overall binding affinity. This might be a consequence of the fact that the introduction of electron-withdrawing groups (*i.e.*, substituents with high Hammett's substituent constant) into planar rings increases their intercalation affinity to DNA. In addition, the observed trend would explain the higher DNA overall damage induced by chloroharmines when compared with Ha (Figure 1).

Table 1. Summary of βCs/ctDNA interaction parameters: K_{SS} represents the slope of the steady-state Stern-Volmer plot. Φ_Δ and Φ_{H2O2} are the quantum yield of singlet oxygen and hydrogen peroxide production, respectively. K_a is the dissociation constant of the dominant acid-base equilibrium observed in aqueous solutions, under physiological pH conditions.

Compound	pK_a	K_{SS} / Mbp^{-1} 10^3				[a, b] Φ_Δ	[a, c] Φ_{H2O2} / 10^{-3}	
		pH 4.8	pH 7.4	pH 8.2	pH 9.5	pD 4.8	pH 4.8	pH 9.0
Ha	[e] 7.5, [f] 7.73 (± 0.03), [g] 7.7, [h] 8.0	17.9 ± 0.1	7.7 ± 0.2	3.3 ± 0.2	[i] 4.6	0.22 ± 0.02	0.84	0.37
6-Cl-Ha	[a, c] 6.3 (± 0.2), [d] 7.58 (± 0.02)	21.3 ± 0.4	[j] 14.7 ± 0.8	12.0 ± 0.6	3.6 ± 0.7	0.19 ± 0.03	1.79	0.76
8-Cl-Ha	[a, c] 6.4 (± 0.2)	18.7 ± 0.1	7.5 ± 0.2	--	--	0.22 ± 0.04	0.77	nd
6,8-diCl-Ha	[a, c] 5.4 (± 0.4)	19.7 ± 0.6	2.1 ± 0.2	--	3.7 ± 0.2	0.05 ± 0.02	1.90	nd

View Article Online
DOI: 10.1039/C8OB00162F

nd: values not determined. [a] Values from Ref [7]. [b, c and d] Values measured in air-equilibrated D_2O, H_2O and phosphate buffer solutions, respectively. [e, f, g, and h] Data obtained from Ref. [6], [56], [57] and [58], respectively. [i] Values from Ref [14], measured in air-equilibrated aqueous solutions at 9.5-10.0. [j] Value obtained from the initial linear portion of the curve.

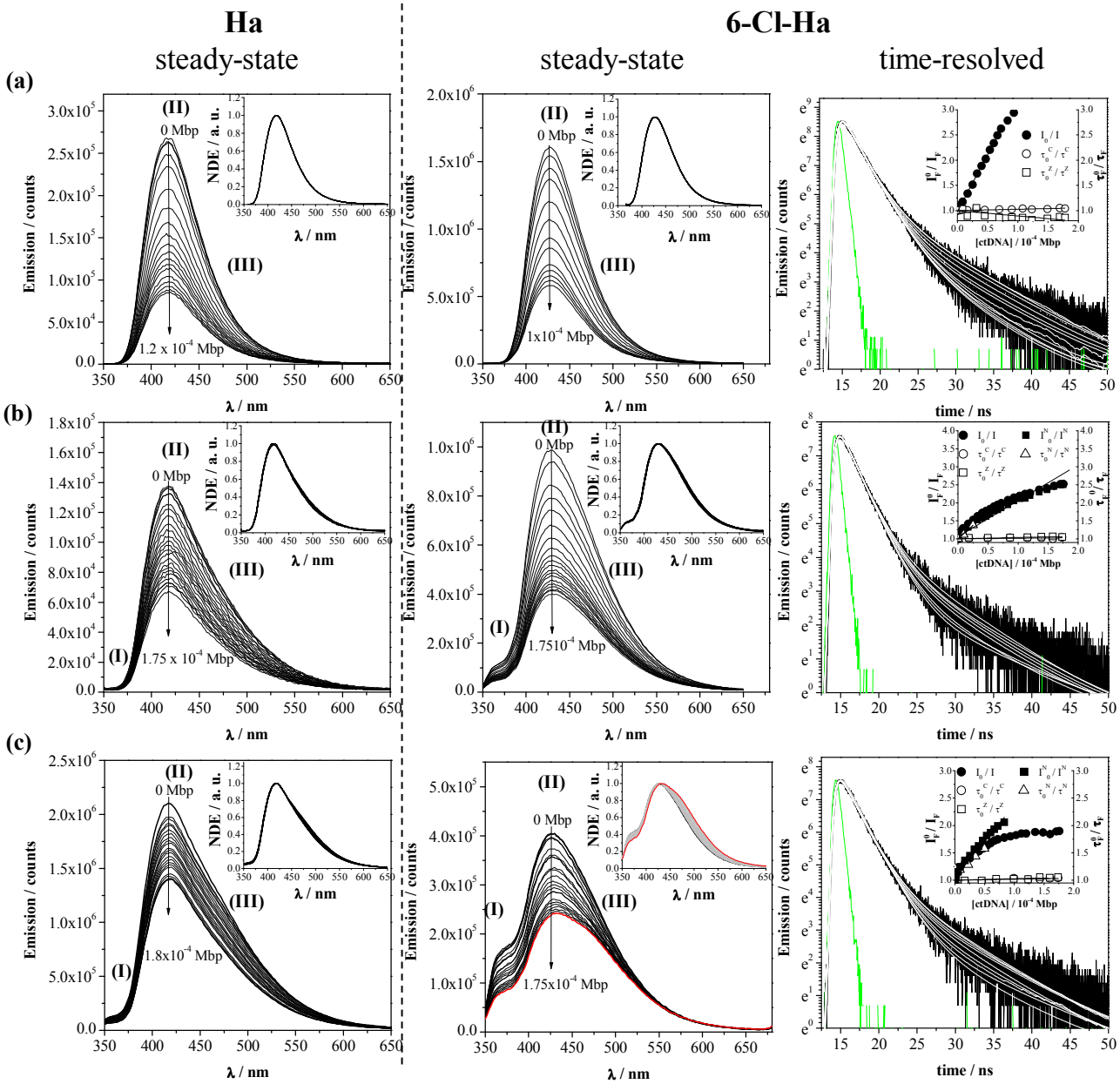

Figure 4. Corrected fluorescence emission spectra of Ha (*left column,* λ_{exc} = 344 nm) and 6-Cl-Ha (*middle column*, λ_{exc} = 340 nm) buffered solution (11.5 μM) recorded in the presence of increasing amounts of ctDNA at pH: **(a)** 4.8, **(b)** 7.4 and **(c)** 8.2. Arrows indicate the variation in [ctDNA] (Mbp). (I), (II) and (III) correspond to the emission bands of **N***, **C*** and **Z*** species of 6-Cl-Ha, respectively. *Insets in left and middle columns*: Normalized Emission (NE) spectra. *Right column*: fluorescence decay of 6-Cl-Ha recorded in air-equilibrated buffered solutions at different pH values (black lines. λ_{exc} = 341 nm and λ_{em} = 428 nm), prompt signal (green line) and bi-exponential fitting curves (white lines). *Insets in right column*: Stern–Volmer plots of the fluorescence intensities (I_F) and lifetimes (τ_F). I_F (black circles) represents the total emission calculated as the integral below the whole emission spectra, whereas I_F^N (black squares) represents emission counts at λ_{em} = 370 nm (λ_{exc} = 341 nm).

View Article Online
DOI: 10.1039/C8OB00162F

Molecular mechanism of SSBs generation by photoexcited 6-Cl-Ha

Time-resolved fluorescence: dynamic interaction of photo-excited 6-Cl-Ha and ctDNA

The quite distinctive spectroscopic behaviour described above for the interaction of 6-Cl-Ha with DNA was further investigated by time-resolved fluorescence spectroscopy. Briefly, time-resolved decays were recorded at representative wavelength nearby the emission maximum of **N***, **C*** and **Z*** 6-Cl-Ha's emitting species (*i.e.*, 360 nm, 430 nm and 510 nm). All the samples were excited using a NanoLED source at 341 nm.

To begin with, the dynamic fluorescence behaviour of 6-Cl-Ha in buffered solutions was investigated to further assign and/or confirm the photo-excited species present under these experimental conditions. All decay curves showed a bi-exponential behaviour (Figure SI.10). This is expected due to the overlapped emission spectra of the fluorescent species (Figure SI.6b) that might contribute to the signal at the monitoring wavelength (λ_{em}) [59]. Under the three pH conditions, lifetime values (τ) for **C*** and **Z*** were determined to be ~2 ns and ~12 ns, respectively, whereas under neutral and low-alkaline conditions a third lifetime of ~0.4 ns was obtained for **N*** (Table SI.1 in Supporting Information). These data are the same, within the experimental error, to those observed for 6-Cl-Ha in pure water (*i.e.*, 2.2 ns, ~0.4 ns and 8.5-12 ns for **C***, **N*** and **Z***, respectively) [7].

Note that the presence of the relative long-lived species, corresponding to **Z***, was also confirmed in both acetate and borax buffered solutions. This fact represents an additional qualitative difference with respect to the dynamic behaviour of 6-Cl-Ha described in acidic aqueous solution (free of buffer) where a single emitting species was observed (Figure SI.10).

On the other hand, the lack of dependence of τ values on the pH- and solvent (buffer) shows no preferential dynamic deactivation of photoexcited 6-Cl-Ha by the anions present in the solutions. Therefore, the relative increase of **Z*** observed in buffered solutions with respect to pure water (Figure SI.6b) might be a consequence of a static quenching of **C** by the anions present in buffered solutions.

In the presence of ctDNA, although fluorescence decays curves of 6-Cl-Ha showed the above described bi-exponential pattern (Figures 4, SI.11 and SI.12), each acid-base species (**N***, **C*** and **Z***) showed a quite distinctive dynamic interaction with ctDNA. Briefly, in the whole pH-range

View Article Online
DOI: 10.1039/C8OB00162F

investigated, τ_F values assigned to **C*** (~2 ns) and **Z*** (~12 ns) showed a small decrease. This decrease was quantified by time-resolved Stern-Volmer plots (Figure 4) of τ_F data as a function of [ctDNA] used, that showed slopes of $K_D = k_q \tau_0 \sim 10^2$ Mbp^{-1} (Table 2) [60], yielding in turn quenching rate constant values of $k_q \sim 10^{10} - 10^{11}$ Mbp^{-1} s^{-1}. It is worth mentioning that K_D values shown by **C*** and **Z*** are two orders of magnitude lower than the slope of the Stern-Volmer plot obtained from the independent steady-state experiment ($K_{SS} = I_0 / I \sim 10^4$ Mbp^{-1}, Tables 1 and 2). This fact indicates that, as it was demonstrated for other related βC derivatives [14], **C** mainly interact with ctDNA trough the formation of a static complex in their electronic ground state.

On the contrary, at pH 7.4 and 8.2, ctDNA induces a quite strong deactivation of **N*** fluorescence lifetime. The Stern-Volmer constant obtained from this data ($K_D = k_q \tau_0^N \sim 10^4$ Mbp^{-1}) is entirely consistent with that obtained from the independent steady-state experiment (I_0^N / I^N) (see black squares in Figure 4), and yields a quenching rate constant of $k_q \sim 10^{13}$ Mbp^{-1} s^{-1}. Such a dynamic deactivation could be accounted by a proton transfer reaction between **N*** and ctDNA (Scheme 3).

Table 2. Summary of βCs/ctDNA interaction dynamic parameters: K_D represents the slope of the time-resolved Stern-Volmer plot, $<\tau_F>$ is the βC's average fluorescence lifetime value observed in the absence of ctDNA and k_q is the bimolecular quenching rate constant ($k_q = K_D / <\tau_F>$). K_{SS} values taken from Table 1 are also listed for comparative purpose.

	pH 4.8				pH 7.4				pH 8.2			
Compound	K_{SS} / 10^3 Mbp^{-1}	K_D / 10^3 Mbp^{-1}	$<\tau_F>$ / ns	k_q / Mbp^{-1} s^{-1}	K_{SS} / 10^3 Mbp^{-1}	K_D / 10^3 Mbp^{-1}	$<\tau_F>$ / ns	k_q / Mbp^{-1} s^{-1}	K_{SS} / 10^3 Mbp^{-1}	K_D / 10^3 Mbp^{-1}	$<\tau_F>$ / ns	k_q / Mbp^{-1} s^{-1}
Ha	17.9 ± 0.1	[b] 0.54 ± 0.02	7.06 (C)	7.6 x 10^{10}	7.7 ± 0.2	nd	nd		7.7 ± 0.3	[c] 0	0.44 (N) 6.96 (C)	
6-Cl-Ha	21.3 ± 0.4	-- 0.27 ± 0.03 (C) -0.05 ± 0.05 (Z)	-- 2.0 ± 0.1 (C) 12.0 ± 0.2 (Z)	1.4 (± 0.2) x 10^{11} --	14.7 ± 0.8	14.9 ± 0.3 (N) 0.15 ± 0.05 (C) 0.36 ± 0.05 (Z)	0.4 ± 0.2 (N) 2.0 ± 0.1 (C) 11.0 ± 0.1 (Z)	3.7 (± 0.8) x 10^{13} 8 (± 3) x 10^{10} 3.3 (± 0.5) x 10^{10}	12.0 ± 0.6	10.3 ± 0.8 (N) 0.18 ± 0.05 (C) 0.28 ± 0.03 (Z)	0.4 (± 0.2) (N) 2.2 (± 0.1) (C) 12.4 (± 0.4) (Z)	3 (± 1) x 10^{13} 8.2 (± 0.8) x 10^{10} 2.3 (± 0.3) x 10^{10}

nd: values not determined.

View Article Online
DOI: 10.1039/C8OB00162F

Multivariate analysis of absorption and fluorescence data obtained for 6-Cl-Ha

The distinctive spectroscopic behaviour of 6-Cl-Ha observed in the presence of ctDNA was further analysed by multivariate analysis of absorption and fluorescence data. Three different types of data matrices (D_{Em}, D_{Ab} and D_{Ex}) were constructed by collecting the emission, absorption and excitation spectra of 6-Cl-Ha solutions under different experimental conditions (pH and [ctDNA]). Details are provided as supplementary information.

Absorption, excitation and emission spectra of all the species present in the investigated systems under different pH values and ctDNA concentrations were deconvoluted by multivariate analysis (Figure 5) and subsequently assigned to different 6-Cl-Ha species (Section 14, SI). Briefly in the absence of DNA, two major species (**N** and **C**) contribute to the overall absorption/excitation processes, whereas emission spectra can be properly described by three major independent contributions (**N***, **C*** and **Z***). It is worth noting that additional very minor contributions (< 5.5% for the entire sample set, and practically independent of the sample pH) ascribed to **A** and **A***, were needed explain the overall excitation and emission spectra, respectively.

On the other hand, in the presence of different [ctDNA], besides **C** and **N** (and **A**, as a minor contribution) an extra independent contribution was required in order to properly describe absorption and excitation experimental data matrices (D_{Ab} and D_{Ex}). Noteworthy, the additional contribution observed in the presence of ctDNA, which resembles the spectrum of **C** although somewhat red shifted (~ 10 nm), exhibits important absorptions at wavelengths where ctDNA absorption can be considered negligible. Moreover, curve resolution of absorbance data matrices shows that the spectral contribution of the additional species increases with [ctDNA] (Figure SI.13a). This provides strong evidence of the formation of a non-emitting "static complex" between the ground state of the cationic species of 6-Cl-Ha (**C**) and ctDNA, probably a donor-acceptor complex stable in both ground and electronic excited states. This finding supports the proposed electrostatic interaction between the **C** and the ctDNA (Figure 5c).

Noteworthy, in the presence of ctDNA, the shapes of the resolved emission spectra remain unchanged and can also be properly described by the spectral contributions shown in Figure 5a, suggesting that the nature of the emitting species is not affected by the presence of ctDNA. In this context, it is worth mentioning that, despite the presence of ctDNA did not affect the shapes of the emission spectra, the contributions on **C***, **Z***, **N*** and **A*** decrease as [ctDNA] is increased. Moreover, MCR-ALS analysis shows that the relative contribution of **Z*** increases with respect to the other 6-Cl-Ha excited species, due to the presence of ctDNA. The latter fact is consistent with

View Article Online
DOI: 10.1039/C8OB00162F

proton transfer reactions between photoexcited 6-Cl-Ha with ctDNA and H_2O, yielding βC(Z*), ctDNA-H^+ and OH^-.

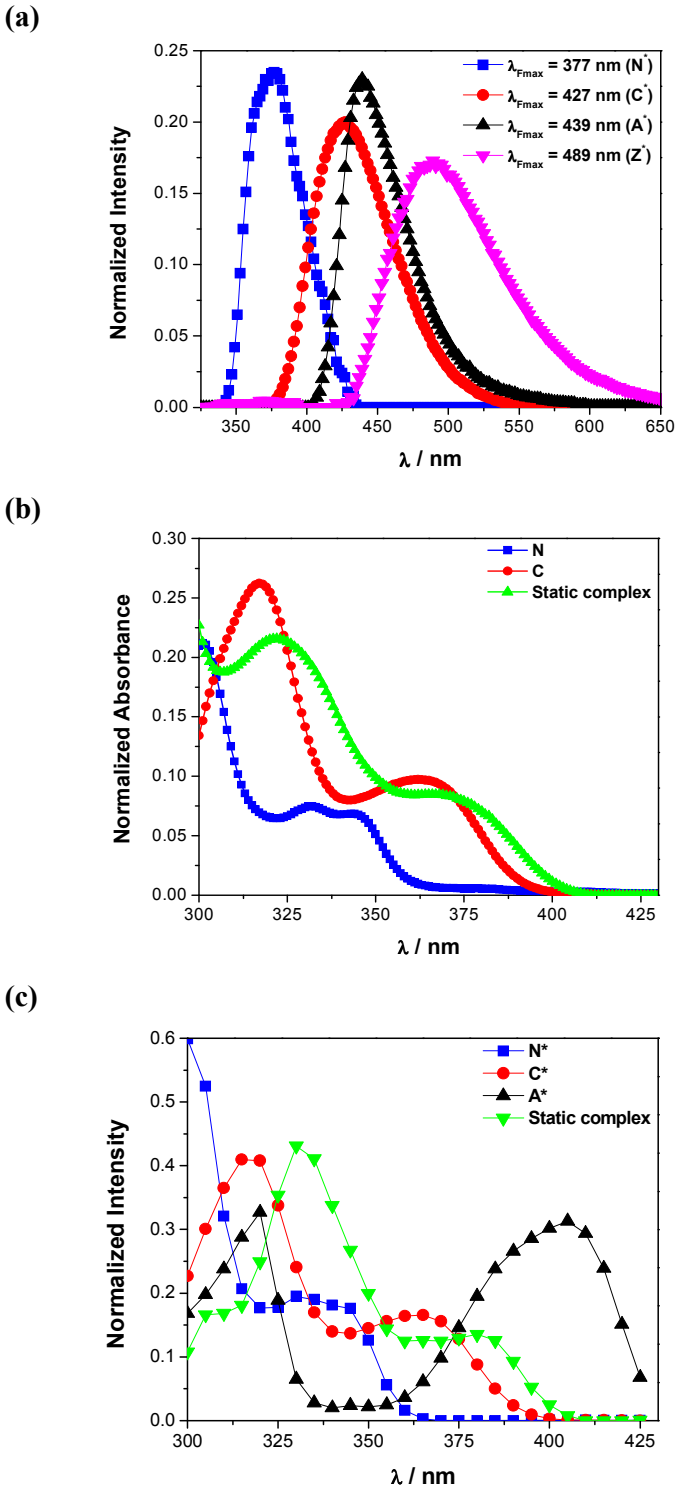

Figure 5. Normalized spectra of 6-Cl-Ha species retrieved form MCR-ALS analysis of D_{Em}, D_{Ab} and D_{Ex} matrices containing spectroscopic data recorded at different pH conditions and [ctDNA] **(a)** Emission profiles **(b)** Absorption profiles **(c)** Excitation profiles.

View Article Online
DOI: 10.1039/C8OB00162F

pH-dependence on the DNA-endonuclease-sensitive modifications induced by 6-Cl-Ha

To further explore the quite unique behaviour of 6-Cl-Ha, among all the β-carbolines investigated, we analysed the contribution of the different 6-Cl-Ha' acid-base species (*vide supra*) on the PM2 damage. To this end, the number of SSB and Fpg-sensitive modifications photoinduced by 6-Cl-Ha was measured under different pH-conditions (Figure 6a). Results shown in Figure 6a clearly indicate that the ratio "SSB/Fpg-sensitive modifications" increases with the pH (*i.e.*, the higher the relative concentration of **N** and, in consequence, the steady-state concentration of **N***, the higher the SSBs formation). For a direct comparison, normalized data are depicted in Figure SI.14. At pH 5.5, the number of Fpg-sensitive sites was clearly higher than that of SSBs, but too high to be accurately quantified. In the relaxation assay, the supercoiled form of the PM2 DNA was no longer detectable after incubation with Fpg-protein, and linearized DNA was formed, indicating frequent incisions.

The above-mentioned pH-effect not only applies for SSBs, but also for AP-sites. This is evident from the fact that the Fpg-sensitive sites detected are mostly AP sites (sensitive to both Fpg and endonuclease IV) (Figures 2 and SI.15). Also, it is accounted for by the increase in the relative SSBs and AP-sites (quantified by endonuclease IV) concentrations without changing the DNA damage profile induced by all the other endonucleases at pH 8.1 (Figure SI.15), with respect to pH 7.4 (Figure 2). The time dependence analysis (Figure SI.16) shows that, even under alkaline conditions (pH 8.1 and 8.7), SSBs are not generated as secondary lesions from Fpg-sensitive precursor lesions. Thus, the high number of SSBs appears to be formed through a photosensitizing pathway that is different from that giving rise to the Fpg-sensitive modifications (*vide infra*).

The lack of any significant scavenging- and/or D_2O-effect on the DNA damage profile suggests that, even under alkaline conditions (Figures 8b and c), neither ROS nor other reactive radical species (*i.e.*, $Cl^{\bullet}$) play a relevant role in the overall DNA-photodamage. As it was observed before in experiments performed at neutral pH (Figure 3a), D_2O solvent only induces a quite small increase in the relative number of Fpg-sensitive sites and causes no changes in the numbers of SSBs as well as AP-sites (Figure 6b).

View Article Online
DOI: 10.1039/C8OB00162F

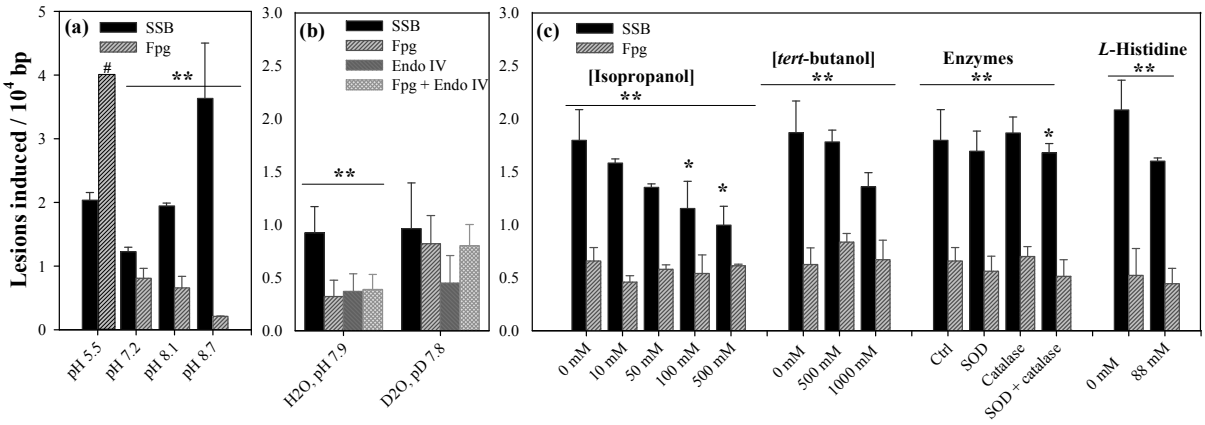

Figure 6. SSB and endonucleases sensitive modifications induced in PM2 DNA by photo-excited 6-Cl-Ha (20 μM) exposure to 20 min of UVA light (365 ± 20 nm) in: **(a)** H_2O under different pH conditions (# indicates data out of range). **(b)** H_2O and D_2O aqueous media at pH and pD 7.9 and 7.8, respectively, and **(c)** H_2O, at pH 8.1, in the presence of increasing amount of selective ROS scavengers. All data depicted are the means of 4 independent experiments (± S.D). * indicates statistically significant differences in each DNA modifications (SSB or Fpg) between samples irradiated in the presence of scavengers and their corresponding controls ($p < 0.05$, ANOVA / Dunnett´s tests). ** indicates statistically significant differences between SSBs and Fpg-sensitive modifications within each experimental condition ($p < 0.05$, t-tests).

It is noticeable that only a small decrease in the number of SSBs as well as of AP-sites (Figure 6c and SI.15) can be observed when DNA photosensitization takes place in the presence of high isopropanol concentrations. The absence of a scavenging effect is a strong indication that reactive radical species are not involved in DNA damage. On the contrary, hydrolytic attack could be a reasonable reaction pathway that might explain SSBs and AP-sites formation, where the photoexcited-βC would play a key role due to its dual acid-base behaviour (*i.e.*, it can be both a quite strong Lewis base as well as a non-negligible Brønsted–Lowry acid as well).

The decrease in the number of SSBs as a function of the isopropanol concentration is more evident under low-alkaline conditions (pH 8.1) (Figures 6c and SI.15) than at neutral pH (Figure 3b), which is highly probable due to the change in the relative steady-state concentration of the photo-excited 6-Cl-Ha acid-base species. This is further supported by the emission spectra of 6-Cl-Ha recorded in the presence of increasing amounts of isopropanol (Figure SI.17). Briefly, a relative decrease in **N*** and **C*** is observed, while **Z*** (or **A***) steady-state concentration is increased.

When DNA damage is evaluated in the presence of a weak base such as *L*-histidine (pK_a of the imidazole ring = 6.0), the reduction in the number of SSBs is statistically relevant (Figures 8c). Moreover, *L*-histidine also induces the same pattern of changes on the 6-Cl-Ha fluorescence emission profile (Figure SI.17), leading to a relative decrease in **N*** and **C***, increasing at the same time the steady-state concentration of **Z*** (or **A***).

View Article Online
DOI: 10.1039/C8OB00162F

Mechanism suggested for the generation of SSBs by photo-excited 6-Cl-Ha

In summary, our data indicate that a decrease in the steady-state concentration of **N*** leads to a decrease in the yield of SSBs and AP-sites and give evidence that ROS do not play any significant role in the generation of these types of DNA damages. Moreover, **N*** appears to be involved in proton transfer processes with DNA moiety. Our findings support the notion that SSBs and AP sites are the result of concerted and stereospecific hydrolysis of phosphodiester bonds photoinduced by 6-Cl-Ha, as a consequence of the intrinsic βC capability of participating in proton-transfer processes, which cause a drastic change in the local [H^+] of the DNA molecule:

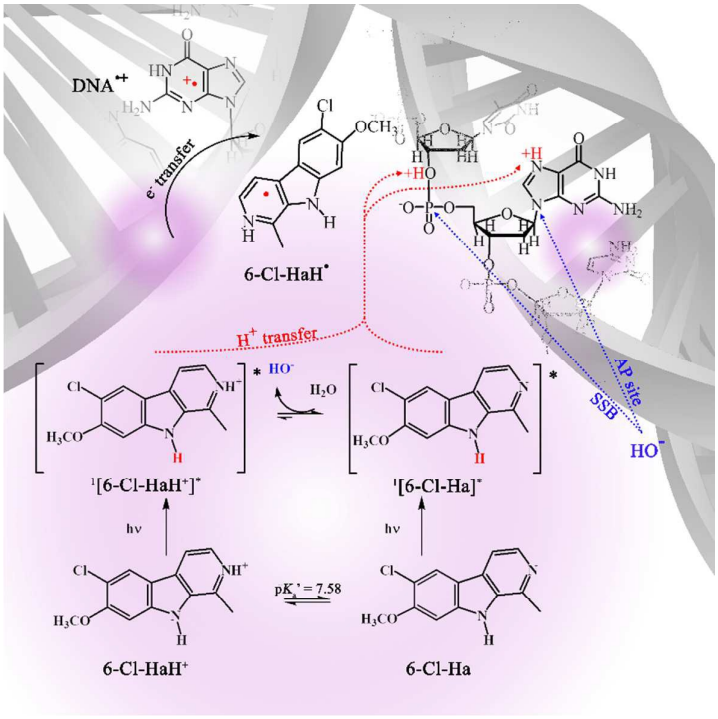

Scheme 3. Main photochemical pathways involved in the DNA damage photosensitized by 6-Cl-Ha. Upon photoexcitation, either neutral ([6-Cl-Ha]*) or cationic ([6-Cl-HaH^+]*) species participate in H+-transfer processes (in red) to DNA that become more sensitive to hydrolytic attack. In addition, upon photoexcitation, [6-Cl-Ha]* induces OH^-formation, *i.e.*, the hydrolytic species, giving rise to the formation of SSBs or AP-sites (in blue). Alternatively, electron transfer reactions might takes place between photoexcited cationic species ([6-Cl-HaH^+]*) and DNA, leading to purine nucleobases photooxidation (top left, in black).

CONCLUSIONS

A number of key issues have been addressed in this study. To begin with, under physiological pH, photoexcited chloroharmines are quite efficient DNA photosensitizers. Photoinduced damage profile depends on the chemical structure of the chloroharmine derivative. The analysis with repair enzymes revealed that oxidatively generated purine modifications such as 8-oxo-7,8-dihydroguanine and AP-sites are generated when 8-chloro-substituted harmines (*i.e.*, 8-Cl-Ha and 6,8-diCl-Ha) are used as photosensitizers. On the contrary, 6-Cl-Ha shows a quite unique

View Article Online
DOI: 10.1039/C8OB00162F

behaviour, leading to the formation of single-strand breaks (SSBs) and AP-sites via a concerted and stereospecific hydrolytic attack as a consequence of a deep change in the local H^+ and OH^- concentration in the surroundings of DNA chain.

To our knowledge, the latter case would represent an exception to the general sensitizing reactions, including those described for artificial nucleases and photonucleases. Nucleases include redox-active coordination complexes that nick DNA under physiological conditions by oxidative attack on the ribose or deoxyribose moiety. [61, 62] The vast majority of photonucleases described in the literature are mainly based on transition metals complexes [63-69] and a group of heterocyclic macrocycle organic compounds (such as chlorophyll and corrole derivatives, etc.)[70, 71] that induce DNA photooxidative cleavage through type I or type II (or a combination of both) reactions, with the concomitant degradation of the photonuclease and/or DNA bases and/or deoxyribose photooxidation. In this context, 6-Cl-Ha may provide an interesting and important perspective on DNA photocleavage as a "clean" artificial photonuclease.

The relevance of the understanding of the molecular bases of the DNA lesions induced by exogenous and/or endogenous photosensitizers is enhanced by its strong impact on human health, due to its direct linkage with mutagenesis and carcinogenesis. As well, from a biomedical point of view, the controlled and selective production of lesions is a promising tool for the design and development of novel photo-therapeutic agents and strategies for their application. As is known, PDT is usually performed via type II photosensitization (*i.e.*, inducing singlet oxygen production). This fact represents a clear limitation of its application to diseases that exhibit hypoxia conditions such as solid tumors [72]. In this context, the use of long wavelength absorbers (via TPA) capable of performing type I photosensitization and/or DNA hydrolytic attack, such as chloroharmines, could be seen as a way to tackle both hypoxic conditions and the need of relatively penetrating radiations [73].

Supporting Information Available. Optimized molecule structure of 8-Cl-Ha and Ha, Time-dependence study of the PM2 damage induced by different concentration of photo-excited 6-Cl-Ha, in phosphate (pH 7.4) buffer solutions; thermal stability of 8-Cl-Ha and 6,8-diClHa in phosphate (pH 7.4) buffer solutions; SSB modifications induced on DNA by photo-excited Ha, PNS and RB; spectrophotometric titration of 6-Cl-Ha in phosphate buffer solution. UV-visible and fluorescence emission spectra of chloroharmines in buffer solutions. MRC-ALS analysis; quenching of Ha, 8-Cl-Ha and 6,8-diCl-Ha fluorescence by ctDNA; fluorescence decays and lifetimes of 6-Cl-Ha in buffer solutions; quenching of fluorescence 6-Cl-Ha by ctDNA at pH 7.4 and 8.1; Multivariate analysis of absorption and emission data obtained for 6-Cl-Ha; Normalized damage profile induced by 6-Cl-Ha

View Article Online
DOI: 10.1039/C8OB00162F

under different pH conditions; damage profile induced by 6-Cl-Ha at pH 8.1, in the presence of isopropanol; time-dependence study of the SSBs and Fpg-sensitive base modifications photoinduced by 6-Cl-Ha in phosphate buffer solution at pH 8.1 and 8.7 and effect of isopropanol and L-histidine on 6-Cl-Ha (pH 8.1); and UV-visible absorption and fluorescence emission spectra. All this material is available free of charge via the Internet at xx.

ACKNOWLEDGEMENTS

The present work was partially supported by ANPCyT (PICT 2015-0374 and 2013-2536), UBA (X088) and UNSAM (E103). JGY and FAORS thank CONICET for doctoral and postdoctoral research fellowships, respectively. MPD, FSGE, REB and FMC are research members of CONICET. Authors thank C. G. Alberici (CONICET) for his technical support.

NOTES AND REFERENCES

1. D. E. J. G. J. Dolmans, D. Fukumura and R. K. Jain, *Nat Rev Cancer*, 2003, **3**, 380-387.
2. A. P. Castano, P. Mroz and M. R. Hamblin, *Nat Rev Cancer*, 2006, **6**, 535-545.
3. P. Agostinis, K. Berg, K. A. Cengel, T. H. Foster, A. W. Girotti, S. O. Gollnick, S. M. Hahn, M. R. Hamblin, A. Juzeniene, D. Kessel, M. Korbelik, J. Moan, P. Mroz, D. Nowis, J. Piette, B. C. Wilson and J. Golab, *CA: A Cancer Journal for Clinicians*, 2011, **61**, 250-281.
4. L. K. McKenzie, I. V. Sazanovich, E. Baggaley, M. Bonneau, V. Guerchais, J. A. G. Williams, J. A. Weinstein and H. E. Bryant, *Chemistry – A European Journal*, 2017, **23**, 234-238.
5. M. M. Gonzalez, M. L. Salum, Y. Gholipour, F. M. Cabrerizo and R. Erra-Balsells, *Photochemical & Photobiological Sciences*, 2009, **8**, 1139-1149.
6. M. M. Gonzalez, J. Arnbjerg, M. Paula Denofrio, R. Erra-Balsells, P. R. Ogilby and F. M. Cabrerizo, *Journal of Physical Chemistry A*, 2009, **113**, 6648-6656.
7. F. A. O. Rasse-Suriani, M. Paula Denofrio, J. G. Yañuk, M. Micaela Gonzalez, E. Wolcan, M. Seifermann, R. Erra-Balsells and F. M. Cabrerizo, *Physical Chemistry Chemical Physics*, 2016, **18**, 886-900.
8. F. A. O. Rasse-Suriani, F. S. García-Einschlag, M. Rafti, T. Schmidt De León, P. M. David Gara, R. Erra-Balsells and F. M. Cabrerizo, *Photochemistry and Photobiology*, 2018, **94**, 36-51.
9. F. M. Cabrerizo, J. Arnbjerg, M. P. Denofrio, R. Erra-Balsells and P. R. Ogilby, *ChemPhysChem*, 2010, **11**, 796-798.
10. M. Vignoni, F. A. O. Rasse-Suriani, K. Butzbach, R. Erra-Balsells, B. Epe and F. M. Cabrerizo, *Organic & Biomolecular Chemistry*, 2013, **11**, 5300-5309.
11. M. M. Gonzalez, M. P. Denofrio, F. S. Garcia Einschlag, C. A. Franca, R. Pis Diez, R. Erra-Balsells and F. M. Cabrerizo, *Physical Chemistry Chemical Physics*, 2014, **16**, 16547-16562.
12. M. M. Gonzalez, F. A. O. Rasse-Suriani, C. A. Franca, R. Pis Diez, Y. Gholipour, H. Nonami, R. Erra-Balsells and F. M. Cabrerizo, *Organic and Biomolecular Chemistry*, 2012, **10**, 9359-9372.
13. M. M. Gonzalez, M. Pellon-Maison, M. A. Ales-Gandolfo, M. R. Gonzalez-Baró, R. Erra-Balsells and F. M. Cabrerizo, *Organic and Biomolecular Chemistry*, 2010, **8**, 2543-2552.
14. M. M. Gonzalez, M. Vignoni, M. Pellon-Maison, M. A. Ales-Gandolfo, M. R. Gonzalez-Baro, R. Erra-Balsells, B. Epe and F. M. Cabrerizo, *Organic and Biomolecular Chemistry*, 2012, **10**, 1807-1819.
15. G. M. Olmedo, L. Cerioni, M. M. González, F. M. Cabrerizo, S. I. Volentini and V. A. Rapisarda, *Frontiers in Microbiology*, 2017, **8**.
16. M. Vignoni, R. Erra-Balsells, B. Epe and F. M. Cabrerizo, *Journal of Photochemistry and Photobiology B: Biology*, 2014, **132**, 66-71.
17. K. Butzbach, F. A. O. Rasse-Suriani, M. M. Gonzalez, F. M. Cabrerizo and B. Epe, *Photochemistry and Photobiology*, 2016, **92**, 611-619.
18. J. G. Yañuk, M. L. Alomar, M. M. Gonzalez, F. Simon, R. Erra-Balsells, M. Rafti and F. M. Cabrerizo, *Physical Chemistry Chemical Physics*, 2015, **17**, 12462-12465.
19. I. Maisuls, E. Wolcan, O. E. Piro, G. A. Etcheverria, G. Petroselli, R. Erra-Ballsels, F. M. Cabrerizo and G. T. Ruiz, *Dalton Transactions*, 2015, **44**, 17064-17074.
20. I. Maisuls, E. Wolcan, O. E. Piro, E. E. Castellano, G. Petroselli, R. Erra-Balsells, F. M. Cabrerizo and G. T. Ruiz, *ChemistrySelect*, 2017, **2**, 8666-8672.
21. B. Epe, *Photochemical and Photobiological Sciences*, 2012, **11**, 98-106.
22. K. S. Gates, *Chemical Research in Toxicology*, 2009, **22**, 1747-1760.
23. J. Cadet, T. Douki and J.-L. Ravanat, *Accounts of Chemical Research*, 2008, **41**, 1075-1083.
24. W. K. Pogozelski and T. D. Tullius, *Chemical Reviews*, 1998, **98**, 1089-1108.
25. J. C. Quada, D. Boturyn and S. M. Hecht, *Bioorganic & Medicinal Chemistry*, 2001, **9**, 2303-2314.
26. B. Armitage and G. B. Schuster, *Photochemistry and Photobiology*, 1997, **66**, 164-170.
27. D. Hrsak, L. Holmegaard, A. S. Poulsen, N. H. List, J. Kongsted, M. P. Denofrio, R. Erra-Balsells, F. M. Cabrerizo, O. Christiansen and P. R. Ogilby, *Physical Chemistry Chemical Physics*, 2015, **17**, 12090-12099.
28. M. A. Ponce, O. I. Tarzi and R. Erra-Balsells, *Journal of Heterocyclic Chemistry*, 2003, **40**, 419-426.
29. M. Salditt, S. N. Braunstein, R. D. Camerini-Otero and R. M. Franklin, *Virology*, 1972, **48**, 259-262.
30. S. Boiteux, T. R. O'Connor, F. Lederer, A. Gouyette and J. Laval, *Journal of Biological Chemistry*, 1990, **265**, 3916-3922.
31. E. Müller, S. Boiteux, R. P. Cunningham and B. Epe, *Nucleic Acids Research*, 1990, **18**, 5969-5973.
32. A. de Juan, R. Gargallo, J. Jaumot and R. Tauler, *Chemometrics and Intelligent Laboratory Systems*, 2005, **76**, 101-110.

View Article Online
DOI: 10.1039/C8OB00162F

33. A. de Juan and R. Tauler, *Analytica Chimica Acta*, 2003, **500**, 195-210.
34. P. J. Gemperline and E. Cash, *Analytical Chemistry*, 2003, **75**, 4236-4243.
35. B. Epe, J. Hegler and P. Lester, in *Methods in Enzymology*, Academic Press, 1994, vol. Volume 234, pp. 122-131.
36. H. E. Krokan, R. Standal and G. Slupphaug, *Biochemical Journal*, 1997, **325**, 1-16.
37. T. Douki, I. Bérard, A. Wack and S. Andrä, *Chemistry – A European Journal*, 2014, **20**, 5787-5794.
38. Douki et. al. have very recently suggested that, although with a very low relative efficiency (~ 3% – 8%), DNA photosensitization can give rise to the formation of C<>C via a distinctive mechanism that would involve the formation of charge-transfer states.
39. P. Miro, V. Lhiaubet-Vallet, M. L. Marin and M. A. Miranda, *Chemistry – A European Journal*, 2015, **21**, 17051-17056.
40. V. Lhiaubet-Vallet, M. C. Cuquerella, J. V. Castell, F. Bosca and M. A. Miranda, *The Journal of Physical Chemistry B*, 2007, **111**, 7409-7414.
41. J. Cadet, K. J. A. Davies, M. H. G. Medeiros, P. Di Mascio and J. R. Wagner, *Free Radical Biology and Medicine*, 2017, **107**, 13-34.
42. H. Yamada, Y. Kitauchi, K. Tanabe, T. Ito and S.-i. Nishimoto, *Chemistry – A European Journal*, 2011, **17**, 2225-2235.
43. C. Bienvenu, J. R. Wagner and J. Cadet, *Journal of the American Chemical Society*, 1996, **118**, 11406-11411.
44. H. Gattuso, V. Besancenot, S. Grandemange, M. Marazzi and A. Monari, *Scientific Reports*, 2016, **6**, 28480.
45. C. Martí, O. Jürgens, O. Cuenca, M. Casals and S. Nonell, *Journal of Photochemistry and Photobiology A: Chemistry*, 1996, **97**, 11-18.
46. E. Gandin, Y. Lion and A. Van de Vorst, *Photochemistry and Photobiology*, 1983, **37**, 271-278.
47. O. I. Tarzi, M. A. Ponce, F. M. Cabrerizo, S. M. Bonesi and R. Erra-Balsells, *Arkivoc*, 2005, **vii**, 295-310.
48. D. Reyman, M. H. Viñas, G. Tardajos and E. Mazario, *The Journal of Physical Chemistry A*, 2012, **116**, 207-214.
49. Note that Z is only present under electronic excitation of these alkaloids due to the change in the electronic distribution and, as consequence, in the relative acidity of the pyridinic and indolic nitrogen of the βC moiety.
50. K. Hayashi, M. Nagao and T. Sugimura, *Nucleic Acids Res.*, 1977, **4**, 3679.
51. B. K. Paul and N. Guchhait, *The Journal of Physical Chemistry B*, 2011, **115**, 11938-11949.
52. Z. Taira, S. Kanzawa, C. Dohara, S. Ishida, M. Matsumoto and Y. Sakiya, *Jap. J. Toxicol. Environ. Health*, 1997, **43**, 83-91.
53. T. Etienne, T. Very, E. A. Perpète, A. Monari and X. Assfeld, *The Journal of Physical Chemistry B*, 2013, **117**, 4973-4980.
54. T. Etienne, H. Gattuso, A. Monari and X. Assfeld, *Computational and Theoretical Chemistry*, 2014, **1040-1041**, 367-372.
55. In the absence of proton transfer between nucleobase and the excited βC, a full intercalation would certainly provide a non-polar microenvironment to the βC moiety that should be reflected in the emission spectra (i.e., by the increase in the emission band of the neutral form, ~ 380 nm). Clearly, this is not our case, as is evidenced by the protonation of the pyridine nitrogen in the electronic excited state, even under alkaline conditions.
56. M. Balón, J. Hidalgo, P. Guardado, M. A. Muñoz and C. Carmona, *Journal of the Chemical Society, Perkin Transactions 2*, 1993, DOI: 10.1039/p29930000099, 99-104.
57. O. S. Wolfbeis and E. Fuerlinger, *Z. Phys. Chem. (Wiesbaden)*, 1982, **129**, 171-183.
58. F. Tomas Vert, I. Zabala Sanchez and A. Olba Torrent, *Journal of Photochemistry*, 1983, **23**, 355-368.
59. Although a tri-exponential decay would be expected from data recorded at λem 430 nm (due to the contribution of N, C and Z), the quite short lifetime of N (close to the sensitivity range of the spectrofluorometer, 200 ps) cannot be resolved from the quite high contribution of C and Z. Thus, even at 430 nm monitoring emission wavelength, good parameters were obtained for the bi-exponential fits.
60. Under acidic conditions, τF of Z* showed a mild increase with the [ctDNA], ranging from 12 ns to 13 ns. This effect could be accounted by a change in the surroundings and/or environment of the fluorophore due to the presence of ctDNA.
61. D. S. Sigman, *Biochemistry*, 1990, **29**, 9097-9105.
62. K. D. Copeland, M. P. Fitzsimons, R. P. Houser and J. K. Barton, *Biochemistry*, 2002, **41**, 343-356.
63. J. Malina, M. J. Hannon and V. Brabec, *Chemistry – A European Journal*, 2008, **14**, 10408-10414.
64. Y. Sun, Y.-J. Hou, Q.-X. Zhou, W.-H. Lei, J.-R. Chen, X.-S. Wang and B.-W. Zhang, *Inorganic Chemistry*, 2010, **49**, 10108-10116.
65. B. de Souza, A. J. Bortoluzzi, T. Bortolotto, F. L. Fischer, H. Terenzi, D. E. C. Ferreira, W. R. Rocha and A. Neves, *Dalton Transactions*, 2010, **39**, 2027-2035.
66. B. Armitage, *Chemical Reviews*, 1998, **98**, 1171-1200.
67. D. Crespy, K. Landfester, U. S. Schubert and A. Schiller, *Chemical Communications*, 2010, **46**, 6651-6662.
68. M. H. Kaulage, B. Maji, S. Pasadi, S. Bhattacharya and K. Muniyappa, *European Journal of Medicinal Chemistry*, 2017, **139**, 1016-1029.
69. L. J. K. Boerner and J. M. Zaleski, *Current Opinion in Chemical Biology*, 2005, **9**, 135-144.
70. H. Taima, A. Okubo, N. Yoshioka and H. Inoue, *Chemistry – A European Journal*, 2006, **12**, 6331-6340.
71. Y.-G. Wang, Z. Zhang, H. Wang and H.-Y. Liu, *Bioorganic Chemistry*, 2016, **67**, 57-63.
72. J. M. Brown, in *Methods in Enzymology*, Academic Press, 2007, vol. 435, pp. 295-321.
73. Y.-C. Zheng, M.-L. Zheng, K. Li, S. Chen, Z.-S. Zhao, X.-S. Wang and X.-M. Duan, *RSC Advances*, 2015, **5**, 770-774.